

## CONTROL OF ELECTRIC AND THERMAL PROPERTIES OF COMPOSITES WITH WHISKERS

G. I. Isakov

UDC 621.318.134:537.638

*The kinetic effects — electric conductivity, thermal emf, and thermal conductivity — were studied at different angles between the directions of electric current, heat flux, and metal microwhiskers in semiconductor–metal eutectic composites where, with oriented crystallization, metal phases in semiconductor matrices are formed in the form of parallel whiskers. It is shown that the kinetic effects in oriented-crystallized eutectic compositions are controllable.*

Composite materials have gained wider use in different branches of industry as compared to homogeneous dielectrics, semiconductors, and metals, and solid solutions of them. Therefore, manufacture of composite materials with specified parameters and control of their electric and thermal properties are of special importance for applications.

Among the large variety of composite materials, composites of the semiconductor–metal type, and, in particular,  $A^3B^5$ –metal, are of special significance for applications due to the possibility of their use as polarization filters of IR radiation [1], galvanomagnetic [2] and thermomagnetic [3] sensors, and tensoresistors [4, 5].

In [6], the possibility of controlling the tensometric parameters of microcomposite eutectics of the semiconductor–metal type is established. It is shown that in eutectics of the semiconductor–superconductor type in both normal and superconducting states electric properties of different specimens made of the same material or one specimen are controllable [7, 8]. In [9], it is shown that the thermal conductivities  $\chi$  of GaSb– $V_2Ga_5$  and InSb–NiSb eutectic compositions are controllable due to their dependence on the growth rate of the compositions. We note that control of the thermal conductivity value due to variation of the growth rate requires the manufacture of different composite ingots. The topicality of control of electric and thermal properties of eutectics of the semiconductor–metal type by simpler methods is beyond question. One of these methods can be variation of the angle  $\beta$  between the direction of electric current  $I$ , heat flux  $W$  (temperature gradient  $\nabla T$ ), and metal whiskers  $X$  that are formed in a semiconductor matrix as a result of oriented crystallization.

A number of works [10–18] are devoted to investigation of classical kinetic and quantum effects in eutectic composites based on  $A^3B^5$ –metal. However, in these works the possibility of control of the electric conductivity, thermal emf, and thermal conductivity of eutectic composites of the semiconductor–metal type by simpler methods was not studied systematically. Proceeding from what was stated above, in the present paper we give original results on control of the electric conductivity  $\sigma$ , thermal emf  $\alpha$ , and thermal conductivity  $\chi$  in the eutectic composites InSb– $Yb_5Sb_3$  and InSb–NiSb at different angles  $\beta$ . It should be noted that we were the first to obtain the eutectic composition InSb– $Yb_5Sb_3$  [19–21].

**Experimental Results.** It should be recorded that the metal phases  $Yb_5Sb_3$  and NiSb in the InSb matrix are formed in the form of long whiskers. Metallographic studies showed that the length of the  $Yb_5Sb_3$  whiskers is about  $L = 200$ – $300 \mu\text{m}$  and the diameter  $d = 1 \mu\text{m}$ . For NiSb crystals,  $L = 70$ – $150 \mu\text{m}$  and  $d = 1 \mu\text{m}$ . In both eutectics, the density of whiskers growing from the area unit is  $N \approx 10^4 \text{ mm}^{-2}$ .

To measure the electric conductivity, thermal emf, and thermal conductivity of eutectic compositions from oriented-crystallized materials, we made five specimens that had the shape of a long parallelepiped with dimensions  $15 \times 3 \times 3 \text{ mm}$ . The specimens were cut such that the angles  $\beta$  between the long axes of the parallelepiped  $Z$  and the crystallization direction  $X$  (direction of the length of the whiskers) had the following values:  $\beta = 0, 20, 45, 70,$  and  $90^\circ$ . In measurement of the electric conductivity  $\sigma$ , thermal emf  $\alpha$ , and thermal conductivity  $\chi$ , the directions of the electric current  $I$  and heat flux  $W$  (or temperature gradient  $\nabla T$ ) were parallel to  $Z$  ( $I\|Z, W\|Z, \nabla T\|Z$ ).

---

Institute of Physics, National Academy of Sciences of Azerbaijan, 33 G. Dzavid Ave., Baku, Az-1143, Azerbaijan; email: gudrat@physics.ab.az. Translated from *Inzhenerno-Fizicheskii Zhurnal*, Vol. 77, No. 5, pp. 171–177, September–October, 2004. Original article submitted May 7, 2004.

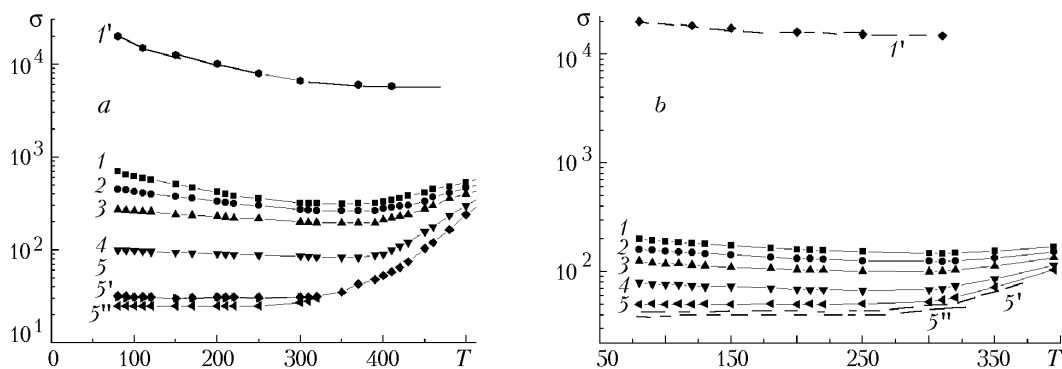


Fig. 1. Temperature dependences of the electric conductivity of the eutectic composites InSb–Yb<sub>5</sub>Sb<sub>3</sub> (a) and InSb–NiSb (b) at different angles  $\beta$  between the directions of electric current and the metal phase: 1)  $\beta = 0^\circ$ ; 2)  $20^\circ$ ; 3)  $45^\circ$ ; 4)  $70^\circ$ ; 5)  $90^\circ$ . Curves 1', calculated values of the electric conductivity of Yb<sub>5</sub>Sb<sub>3</sub> (a) and NiSb (b); 5' and 5'', calculated and experimental values of the electric conductivity of InSb.  $\sigma$ ,  $\Omega^{-1}\cdot\text{cm}^{-1}$ ;  $T$ , K.

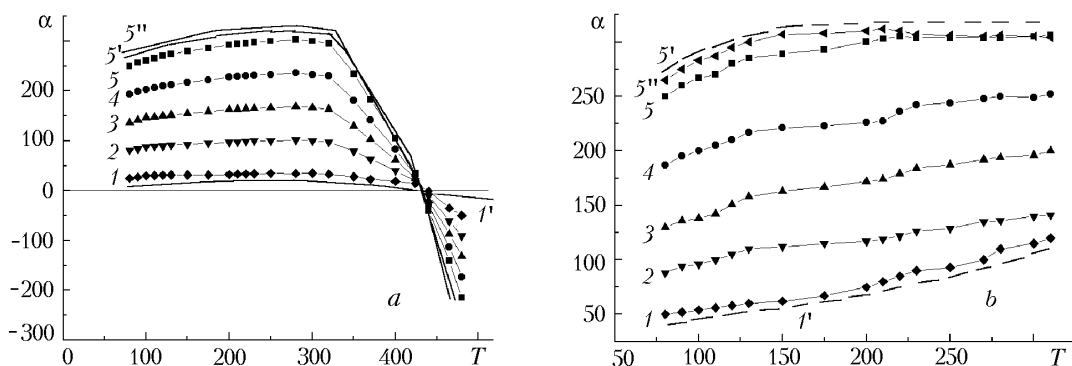


Fig. 2. Temperature dependences of the thermal emf of InSb–Yb<sub>5</sub>Sb<sub>3</sub> (a) and InSb–NiSb (b) at different angles  $\beta$  between the directions of the temperature gradient and the metal phase (for the notation see Fig. 1). Curves 1', calculated values of the thermal emf of Yb<sub>5</sub>Sb<sub>3</sub> (a) and NiSb (b); 5' and 5'', calculated and experimental values of the thermal emf of InSb.  $\alpha$ ,  $\mu\text{V}/\text{K}$ ;  $T$ , K.

Figures 1–3 give the temperature dependences of the coefficients  $\sigma$ ,  $\alpha$ , and  $\chi$  of the eutectic compositions InSb–Yb<sub>5</sub>Sb<sub>3</sub> and InSb–NiSb at different angles  $\beta$ . Depending on the angle  $\beta$  between the directions of  $I$ ,  $W$ , and  $X$ , the following relations are observed for the electric conductivity  $\sigma$ , thermal emf  $\alpha$ , and thermal conductivity  $\chi$  of the eutectic compositions InSb–Yb<sub>5</sub>Sb<sub>3</sub> and InSb–NiSb:

$$\sigma_{\beta=0^\circ} > \sigma_{\beta=20^\circ} > \dots > \sigma_{\beta=90^\circ}, \quad (1)$$

$$\alpha_{\beta=0^\circ} < \alpha_{\beta=20^\circ} < \dots < \alpha_{\beta=90^\circ}, \quad (2)$$

$$\chi_{\beta=0^\circ} > \chi_{\beta=20^\circ} > \dots > \chi_{\beta=90^\circ}. \quad (3)$$

We note that the quantities  $\sigma$  and  $\alpha$  are monitored within the entire studied range of temperatures and as the temperature increases the parameters studied converge.

When  $\beta < 90^\circ$  (Fig. 1, curves 1–4), the electric conductivities of the compositions within the temperature range 80–350 K have the dependence typical of metals. Within the temperature range 300–525 K, the electric conduc-

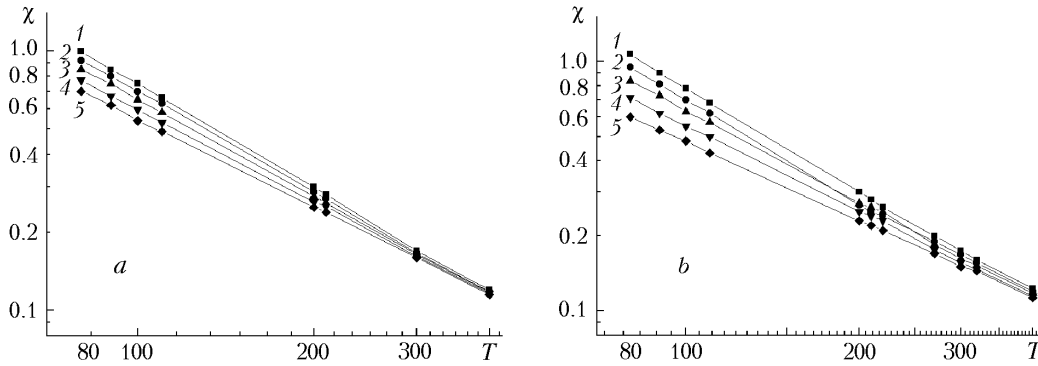


Fig. 3. Temperature dependences of thermal conductivity of InSb–Yb<sub>5</sub>Sb<sub>3</sub> (a) and InSb–NiSb (b) at different angles  $\beta$  between the directions of heat flux and the metal phase (for the notation see Fig. 1).  $\chi$ , V/(cm·K);  $T$ , K.

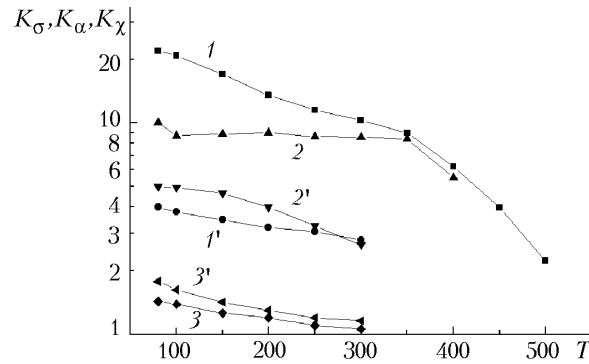


Fig. 4. Temperature dependences of the coefficients of anisotropy of electric conductivity  $K_{\sigma}$  (1, 1'), thermal emf  $K_{\alpha}$  (2, 2'), and thermal conductivity  $K_{\chi}$  (3, 3') of the eutectic composites InSb–Yb<sub>5</sub>Sb<sub>3</sub> (curves 1, 2, and 3) and InSb–NiSb (curves 1', 2', and 3').

tivities of the compositions increase. At  $\beta = 90^{\circ}$  (curves 5), the electric conductivities of the compositions in the temperature range 80–350 K manifest weak semiconductor dependences, whereas in the temperature range 300–525 K these dependences are pronounced.

The coefficient of thermal emf (Fig. 2) also has a strong anisotropy and in the range 80–300 K it increases with an increase in temperature. In the eutectics InSb–Yb<sub>5</sub>Sb<sub>3</sub>, when  $T \geq 330$  K a decrease in  $\alpha$  is observed for all  $\beta$ . At  $T = 430$  K, for all  $\beta$  an inversion of the coefficient of thermal emf  $\alpha$  takes place. It is seen from Fig. 3 that in both eutectics the thermal conductivity  $\chi$  is also anisotropic and when  $T \geq 300$  K curves 1, 2, 3, 4, and 5 converge. At  $T = 400$  K, within the error of thermal conductivity measurement ( $\pm 5\%$ )  $\chi_1 = \chi_2 = \dots = \chi_5$ .

Figures 1 and 2 (curves 5'') present  $\sigma$  and  $\alpha$  of homogeneous InSb with a concentration of holes of  $1.2 \cdot 10^{18} \text{ cm}^{-3}$  and a concentration of electrons of  $1.3 \cdot 10^{16} \text{ cm}^{-3}$ . These values correspond to concentrations of holes of the semiconductor matrix of the eutectic InSb–Yb<sub>5</sub>Sb<sub>3</sub> and concentrations of electrons of the semiconductor matrix of the eutectic InSb–NiSb. We note that the thermal conductivity of homogeneous InSb is in full correspondence with the thermal conductivity of the eutectics InSb–Yb<sub>5</sub>Sb<sub>3</sub> and InSb–NiSb at  $\beta = 0^{\circ}$ ; therefore, it is not given in Fig. 3.

Figure 4 shows the temperature dependences of the coefficients of anisotropy of electric conductivity  $K_{\sigma} = \sigma_{\parallel}/\sigma_{\perp}$  (curves 1 and 1'), thermal emf  $K_{\alpha} = \alpha_{\perp}/\alpha_{\parallel}$  (curves 2 and 2'), and thermal conductivity  $K_{\chi} = \chi_{\parallel}/\chi_{\perp}$  (curves 3 and 3') for the eutectics InSb–Yb<sub>5</sub>Sb<sub>3</sub> and InSb–NiSb, respectively. It is seen from the figure that in both eutectics  $K_{\sigma}$ ,  $K_{\alpha}$ , and  $K_{\chi}$  decrease with an increase in temperature.

**Discussion of Experimental Results.** The strong anisotropy of the electric conductivity and thermal emf of the eutectic compositions InSb–Yb<sub>5</sub>Sb<sub>3</sub> and InSb–NiSb can be explained by shunting of the decreases of voltage  $V_{\sigma}$  and  $V_{\alpha}$  by metal phases, which are formed, respectively, under the effect of the electric field and temperature gradient.

At  $\beta = 0^\circ$ , i.e., when the directions of electric current  $I$  and temperature gradient  $\nabla T$  coincide with the direction of metal inclusions  $X$  ( $I\parallel X, \nabla T\parallel X$ ), the shunting effects of metal microwhiskers are maximum. At  $\beta = 0^\circ$ , the eutectic compositions manifest maximum electric conductivity and minimum thermal emf. This is due to the fact that the coefficient of electric conductivity  $\sigma = (I\Delta l)/(V_\sigma S)$  is inversely proportional, whereas the coefficient of thermal emf  $\alpha = V_\alpha/\nabla T$  is directly proportional to drops of voltages  $V_\sigma$  and  $V_\alpha$ , respectively. In the range  $0^\circ \leq \beta \leq 90^\circ$ , as  $\beta$  increases, the electric conductivity of the eutectic compositions decreases and the thermal emf increases.

It is seen from Fig. 1 that in both eutectics, as is the case of percolation transition of the insulator–metal type, in the temperature range 80–350 K with an increase in  $\beta$  the semiconductor conductivity changes over to metal conductivity in both character and magnitude. This behavior of the conductivity in microcomposite eutectics can be called percolation transition of the semiconductor–metal type. This transition is also observed in Fig. 2 but with decreasing  $\beta$ . At  $\beta = 90^\circ$  (curves 5), the absolute values of the thermal emf are close to the thermal emf of semiconductors, and at  $\beta = 0^\circ$  (curves 1) — to the thermal emf of metals.

The increase in electric conductivity in eutectic compositions within the temperature range 350–500 K is due to transition to the region of intrinsic conductivity of the semiconductor matrix InSb. We note that in both compositions the increase in electric conductivity slows down as  $\beta$  decreases from  $90^\circ$  to  $0^\circ$ . This dependence with an increase in temperature is caused by amplification of two competing mechanisms: increase in electric conductivity due to transition of the semiconductor matrix to the region of intrinsic conductivity and decrease in electric conductivity under the effect of metal phases. In the InSb–Yb<sub>5</sub>Sb<sub>3</sub> composition, the decrease of the coefficient of thermal emf  $\alpha$  below  $T \geq 330$  K is also stipulated by transition to the region of intrinsic conductivity. We note that, in contrast to InSb–NiSb, below 300 K the InSb–Yb<sub>5</sub>Sb<sub>3</sub> composition has a hole conduction. With transition to the region of intrinsic conductivity, electron conduction begins. Simultaneous action of electron and hole mechanisms leads to an increase in electric conductivity and a decrease in thermal emf.

Proceeding from the model of semiconductors connected in parallel and in series, we can determine generalized electric conductivities of semiconductor–metal microcomposite eutectics. According to this model, generalized electric conductivities of oriented-crystallized eutectic compositions at  $I\parallel X$  ( $\beta = 0^\circ, \sigma_{\parallel}$ ) and  $L\perp X$  ( $\beta = 90^\circ, \sigma_{\perp}$ ) are expressed by the following formulas [22]:

$$\sigma_{\parallel} = \sigma_1 \frac{1}{1 + \psi} + \sigma_2 \frac{\psi}{1 + \psi}, \quad (4)$$

$$\sigma_{\perp} = \frac{(\sigma_1 - \sigma_2) \left( 1 - \sqrt{\frac{\psi}{1 + \psi}} \right) + \sigma_2 \sqrt{\frac{1 + \psi}{\psi}}}{1 + \frac{\sigma_2}{\sigma_1} \left( \sqrt{\frac{1 + \psi}{\psi}} - 1 \right)}, \quad (5)$$

where  $\sigma_1$  is the electric conductivity of the semiconductor matrix,  $\sigma_2$  is the electric conductivity of the metal phase, and  $\psi = V_2/V_1$  is the bulk ratio of the metal and semiconductor phases. For the eutectic composition InSb–Yb<sub>5</sub>Sb<sub>3</sub>,  $\psi = 0.037$ , and for InSb–NiSb,  $\psi = 0.013$ . Substituting the values of  $\psi$  into Eqs. (1) and (2) and solving these equations simultaneously, we find  $\sigma_1$  and  $\sigma_2$  within the temperature range 80–500 K. Figure 1 shows the calculated curves of electric conductivity of the semiconductor matrix InSb ( $\sigma_1$ , curves 5') and the metal phase Yb<sub>5</sub>Sb<sub>3</sub> ( $\sigma_2$ , curves 1'). It is seen that the temperature dependence of the calculated electric conductivity  $\sigma_1$  shows a more pronounced metal character than  $\sigma_{\parallel}$  (curves 1) and at  $T = 80$  K  $\sigma_1/\sigma_{\parallel} \approx 28.5$  and  $\sigma_1/\sigma_{\perp} \approx 643$  and at  $T = 400$  K  $\sigma_1/\sigma_{\parallel} \approx 19$  and  $\sigma_1/\sigma_{\perp} \approx 140$ . For InSb–NiSb, at  $T = 80$  K  $\sigma_1/\sigma_{\parallel} \approx 100$  and  $\sigma_1/\sigma_{\perp} \approx 500$ . The decrease in electric conductivity of specimens 1, 2, 3, and 4 within the temperature range 80–300 K shows that they possess a metal character. The semiconductor course of  $\sigma_{\perp}$  is due to the fact that metal whiskers of Yb<sub>5</sub>Sb<sub>3</sub> and NiSb at  $\beta = 90^\circ$  almost do not affect the electric conductivity of the InSb matrix.

Proceeding from what was formulated above, at arbitrary  $\beta$  the formula of control for generalized electric conductivity of semiconductor–metal eutectic compositions can be written as

$$\sigma_{\beta} = \sigma_{\parallel} \sin^2 \beta + \sigma_{\perp} \cos^2 \beta. \quad (6)$$

In the case of heat fluxes that are parallel and perpendicular to the direction of metal phases, thermal emf is expressed by the following formulas [23]:

$$\alpha_{\parallel} = \alpha_1 + \frac{\rho_1 (1 + \psi) (\alpha_2 - \alpha_1)}{\rho_1 (1 + \psi) + \rho_2 (1 + \psi) / \psi}, \quad (7)$$

$$\alpha_{\perp} = \alpha_1 + \frac{\rho_1 \left\{ \alpha_1 \left[ 1 - \left( \frac{\psi}{1 + \psi} \right)^{\frac{1}{2}} \right] + \alpha_2 \left( \frac{\psi}{1 + \psi} \right)^{\frac{1}{2}} \right\} - \alpha_1}{1 - \left( \frac{\psi}{1 + \psi} \right)^{\frac{1}{2}} \left( \rho_1 \left\{ \left[ 1 - \left( \frac{\psi}{1 + \psi} \right)^{\frac{1}{2}} \right]^{-1} + 1 - \left( \frac{\psi}{1 + \psi} \right)^{\frac{1}{2}} \right\} + \rho_2 \right)}. \quad (8)$$

Having substituted the value of  $\psi$  into Eqs. (7) and (8) and solved these equations simultaneously, we find  $\alpha_1$  and  $\alpha_2$  in the temperature range 80–500 K. Figure 2 shows the calculated curves of the semiconductor matrix InSb ( $\alpha_1$ , curves 5') and the metal phase Yb<sub>5</sub>Sb<sub>3</sub> and NiSb ( $\alpha_2$ , curves 1'). It is seen that the calculated temperature dependences of thermal emf  $\alpha_1$  nearly coincide with the experimental values of thermal emf for both InSb (curve 5'') and  $\alpha_{\perp}$ . In specimens 1, 2, 3, and 4 in the temperature range 80–300 K, thermal emf increases. The  $\alpha_2$  determined from Eqs. (7) and (8) manifests a metal behavior and in magnitude it is closer to the thermal emf of metals. The anisotropy of the thermal emf of eutectic semiconductor–metal compositions is due to shunting of the emf of the semiconductor matrix InSb by metal whiskers of Yb<sub>5</sub>Sb<sub>3</sub> and NiSb.

Proceeding from the above, at arbitrary  $\beta$  we write the formula of control for generalized thermal emf as

$$\alpha_{\beta} = \alpha_{\perp} \sin^2 \beta + \alpha_{\parallel} \cos^2 \beta. \quad (9)$$

The generalized thermal conductivity of heterogeneous systems can be expressed by the Odelevskii formulas [24]. For directions that are perpendicular to and parallel with the metal phase, these formulas have the following form:

$$\chi_{\perp} = \chi_1 \left( 1 + \frac{\psi}{\frac{1 - \psi}{2} + \frac{\chi_1}{\chi_2 - \chi_1}} \right), \quad (10)$$

$$\chi_{\parallel} = \chi_1 \left( 1 + \frac{\psi}{\frac{\chi_1}{\chi_2 - \chi_1}} \right),$$

where  $\chi_{\perp}$  and  $\chi_{\parallel}$  are the thermal conductivities of eutectic compositions at  $\beta = 90^\circ$  and  $\beta = 0^\circ$  and  $\chi_1$  and  $\chi_2$  are the thermal conductivities of the semiconductor matrices and metal phases. Substituting the values of  $\psi$  into formulas (10), we can find the thermal conductivities of the semiconductor matrix  $\chi_1$  and the metal phase  $\chi_2$ . It is found that within the measurement error  $\chi_{\perp} \approx \chi_1$  and  $\chi_{\parallel} \approx \chi_1$ . It follows from these expressions that  $\chi_{\perp} \approx \chi_{\parallel}$ . It is seen from the experimental data (Fig. 3) that in the eutectic composition  $\chi_{\parallel} \approx \chi_0$ , although  $\chi_{\perp} \neq \chi_0$  and  $\chi_{\perp} \neq \chi_{\parallel}$ . The equality  $\chi_{\parallel} \approx \chi_0$  shows that the contribution of metal phases at small  $\psi$  to generalized thermal conductivity is negligible and its value lies within the measurement error of thermal conductivity  $\chi_{\parallel}$ .

With an arbitrary direction the formula of control has the form

$$\chi_{\beta} = \chi_{\perp} \sin^2 \beta + \chi_{\parallel} \cos^2 \beta. \quad (11)$$

We note that the mechanisms of shunting that manifest themselves in electric conductivity and thermal emf are not suitable for description of the anisotropy of thermal conductivity. The longitudinal dimensions of the metal phases  $L$  are much larger than their transverse dimensions ( $L \gg d$ ), and when the heat flux is directed perpendicular to the metal phases ( $\beta = 90^\circ$ ) the heat carriers — phonons — can intensely scatter on the metal phases; therefore, anisotropy of the thermal conductivity  $\chi$  in semiconductor–metal eutectic compositions is due to scattering of phonons on the metal phases. Within the range  $0^\circ \leq \beta \leq 90^\circ$  with perpendicular fall of phonons on the surface of the metal phases the angle of scattering is equal to  $90^\circ$ ; it decreases in proportion to the decrease in  $\beta$ , and at  $\beta = 0^\circ$  phonons slide along the surface of the metal phases.

## CONCLUSIONS

1. It is found that in eutectic composites of the semiconductor–metal type the kinetic effects — electric conductivity, thermal emf, and thermal conductivity — are controllable, depending on the direction of the electric current, the temperature gradient or heat flux, and the direction of metal whiskers.

2. It is revealed that in the eutectic composites of the semiconductor–metal type percolation transitions of the semiconductor–metal type are observed, depending on the angle  $\beta$  between the direction of electric current  $I$ , temperature gradient  $\nabla T$ , and metal phase  $X$ .

3. It is shown that in eutectic composites of the semiconductor–metal type anisotropy of the electric conductivity and thermal emf is due to shunting of the voltage drops formed under the effect of the electric field and temperature gradient. Anisotropy of the thermal conductivity is due to scattering of phonons on the metal phases.

The author would like to express his gratitude to F. M. Gashimzade, Academician of the National Academy of Sciences of Azerbaijan, for useful comments in discussing the work.

## NOTATION

$d$ , diameter of whiskers,  $\mu\text{m}$ ;  $I$ , direction of electric current;  $K_{\sigma} = \sigma_{\parallel}/\sigma_{\perp}$ ,  $K_{\alpha} = \alpha_{\perp}/\alpha_{\parallel}$ , and  $K_{\chi} = \chi_{\parallel}/\chi_{\perp}$ , coefficients of anisotropy of electric conductivity, thermal emf, and thermal conductivity of composites;  $L$ , length of whiskers,  $\mu\text{m}$ ;  $\Delta l$ , length of the specimen between the contacts,  $\text{cm}$ ;  $N$ , density of whiskers,  $\text{mm}^{-2}$ ;  $S$ , cross-sectional area of the specimens,  $\text{cm}^2$ ;  $\nabla T$ , direction of the temperature gradient;  $V_{\sigma}$  and  $V_{\alpha}$ , voltage drops between the contacts,  $\text{V}$ ;  $V$ , volume,  $\text{mm}^3$ ;  $W$ , heat-flux direction;  $X$ , direction of metal whiskers;  $Z$ , direction of the long axis of parallelepiped-shaped specimens;  $\alpha$ , generalized thermal emf of composites,  $\mu\text{V/K}$ ;  $\beta$ , angle between the directions of electric current (heat flux or temperature gradient) and whiskers,  $X$ ;  $\chi$ , generalized thermal conductivity of composites,  $\text{W}/(\text{cm}\cdot\text{K})$ ;  $\rho$ , specific resistance,  $\Omega\cdot\text{cm}$ ;  $\sigma$ , generalized electric conductivity of composites,  $\Omega^{-1}\cdot\text{cm}^{-1}$ ;  $\psi = V_2/V_1$ , bulk ratio of metal and semiconductor phases. Subscripts:  $\parallel$  and  $\perp$  indicate that quantities are measured parallel with and perpendicular to the direction of metal whiskers  $X$ ;  $\beta$ , quantities measured at the given  $\beta$ ; 1, semiconductor matrices; 2, metal whiskers.

## REFERENCES

1. B. Paul, H. Weiss, and M. Wilhelm, Die polarisierende Wirkung von zweiphasigem Indiumantimonid im Ultraroten, *Solid State Electronics*, Pergamon Press, **7**, No. 8, 835–841 (1964).
2. G. N. Evstaf'eva, Study of the dependence of magnetoresistive properties of the InSb–NiSb eutectic alloy on the magnetic field and temperature, *Elektron. Tekh.*, No. 3 (118), 85–88 (1978).
3. O. Mosanov, E. Egennazarov, and O. Ismailov, Study of the transverse Nernst–Etingshausen effect in InSb–NiSb, *Izv. Akad. Nauk TSSR, Ser. Fiz.-Tekh.-Khim. Geol. Nauk*, No. 3, 115–117 (1976).
4. M. I. Aliev, Z. A. Dzhafarov, and A. E. Agasiev, Characteristics of tensoresistors made of GaSb–FeGa eutectic alloy, *Prib. Sist. Upravl.*, No. 2, 27–30 (197).

5. M. I. Aliev, Z. A. Dzhabarov, G. I. Isakov, A. A. Khalilova, and A. T. Eminzade, *The Sensitive Element of a Tensosensor*, USSR Inventor's Certificate No. 1294074 (1986).
6. G. I. Isakov, Control over tensoresistive parameters of the semiconductor–metal eutectic composition, *Pis'ma Zh. Tekh. Fiz.*, **22**, No. 24, 71–74 (1996).
7. G. I. Isakov, Control over superconductivity of the semiconductor–superconductor eutectic, *Pis'ma Zh. Tekh. Fiz.*, **29**, No. 19, 40–47 (2003).
8. G. I. Isakov, Control over electric properties of the semiconductor–superconductor eutectic composition, *Prikl. Fiz.*, No. 6, 45–52 (2003).
9. M. I. Aliev, G. I. Isakov, and É. A. Isaeva, Thermal conductivity of the eutectics InSb–NiSb and GaSb–V<sub>2</sub>Ga<sub>5</sub> obtained at different rates of growth, *Fiz. Tekh. Poluprovodn.*, **30**, No. 10, 1871–1875 (1996).
10. M. I. Aliev, S. G. Abdinova, and S. A. Aliev, Kinetic phenomena in the InSb–NiSb eutectic alloys, *Izv. Akad. Nauk SSSR, Neorg. Mater.*, **10**, No. 5, 823–826 (1974).
11. M. I. Aliev and G. I. Isakov, Electric properties of the eutectic alloy in the InSb–YbSb system, *Izv. Akad. Nauk SSSR, Neorg. Mater.*, **16**, No. 5, 782–786 (1980).
12. M. I. Aliev, G. I. Isakov, and R. M. Dzhabbarov, Electric properties of GaSb and InSb doped by Gd and Yb and the eutectics based on them, in: *Physical Properties of Complex Semiconductors* [in Russian], Nauka, Baku (1982), pp. 15–25.
13. I. G. Isakov, Mobility of charge carriers in the GaSb–V<sub>2</sub>Ga<sub>5</sub> and GaSb–GaV<sub>3</sub>Sb<sub>5</sub> eutectics, *Neorg. Mater.*, **39**, No. 6, 677–685 (2003).
14. I. G. Isakov, Special features of percolation superconductivity of the GaSb–V<sub>2</sub>Ga<sub>5</sub> eutectic, *Neorg. Mater.*, **39**, No. 11, 1295–1300 (2003).
15. G. I. Isakov, Special features of superconductivity in the semiconductor–superconductor eutectic, *Fizika*, **6**, No. 1, 50–52 (2000).
16. H. Weiss, Electromagnetic properties of eutectic composites (a critical review), *Met. Trans.*, **2**, No. 6 (1971).
17. V. S. Vekshina, L. Ya. Krol', V. N. Kuz'min, and A. N. Popkov, Properties of the eutectic alloy InSb–NiSb doped by tellurium, *Izv. Akad. Nauk SSSR, Neorg. Mater.*, **12**, No. 2, 332–333 (1976).
18. A. I. Kostin and V. M. Svetlichnyi, On the mechanism of electron scattering in InSb–NiSb, *Ukr. Fiz. Zh.*, **22**, No. 1, 1723–1725 (1977).
19. G. I. Isakov, Obtaining of the semiconductor-metal eutectic composition with specified properties, in: *Ext. Abstr. of Papers presented at the Xth Nat. Conf. on Crystal Growth* [in Russian], Moscow (2002), p. 606.
20. G. I. Isakov, Anisotropic eutectic compositions with controlled physical properties, in: *Ext. Abstr. of Papers presented at the 2nd Int. Conf. on the Physics of Crystals "Crystal Physics of the XXIst Century" devoted to M. P. Shaskol'skaya* [in Russian], 28–30 October 2003, Moscow (2003), pp. 54–56.
21. M. I. Aliev, G. I. Isakov, and Z. I. Suleimanov, Obtaining of oriented-crystallized eutectic (OE) in the In–Sb–Gd, InSb–Yb system, in: *Proc. All-Union Symp. "Physics of the Strength of Composite Materials"* [in Russian], Leningrad (1980), pp. 26–28.
22. V. V. Leonov, E. N. Chunarev, and Yu. E. Spektor, Determination of electric conductivity in the thermal emf of a two-phase semiconductor, in: *Physico-Chemical Properties in Heterogeneous Systems* [in Russian], Krasnoyarsk (1977).
23. W. K. Liebman and W. K. Miller, Preparation, phase-boundary energies and thermoelectric properties of InSb–Sb eutectic alloys with ordered microstructures, *J. Appl. Phys.*, **34**, No. 9, 2653–2659 (1963).
24. B. I. Odelevskii, Calculation of the generalized conductivity of heterogeneous systems. I. Matrix two-phase systems with non-elongated inclusions, *Zh. Tekh. Fiz.*, **21**, No. 6, 667–677 (1951).